Environmental Science and Pollution Research (2023) 30:117609–117623
https://doi.org/10.1007/s11356-023-30417-8

RESEARCH ARTICLE

Assessment of antimicrobial activity and In Vitro wound healing potential of ZnO nanoparticles synthesized with *Capparis spinosa* extract

Selma Sezen[1] · Muhammed Sait Ertuğrul[2] · Özge Balpınar[2] · Cemil Bayram[3] · Mustafa Özkaraca[4] · Irmak Ferah Okkay[5] · Ahmet Hacımüftüoğlu[6] · Medine Güllüce[7]

Received: 26 July 2023 / Accepted: 8 October 2023 / Published online: 23 October 2023
© The Author(s), under exclusive licence to Springer-Verlag GmbH Germany, part of Springer Nature 2023

Abstract

Agents that will accelerate wound healing maintain their clinical importance in all aspects. The aim of this study is to determine the antimicrobial activity of zinc oxide nanoparticles (ZnO NPs) ZnO nanoparticles obtained by green synthesis from *Capparis spinosa* L. extract and their effect on in vitro wound healing. ZnO NPs were synthesized and characterized using *Capparis spinosa* L. extract. ZnO NPs were tested against nine ATCC-coded pathogen strains to determine antimicrobial activity. The effects of different doses (0.0390625–20 µg/mL) of NPs on cell viability were determined by MTT assay. The effect of ZnO NPs doses (0.0390625 µg/mL, 0.078125 µg/mL, 0.15625 µg/mL, 0.3125 µg/mL, 0.625 µg/mL, 1.25 µg/mL) that increase proliferation and migration on wound healing was investigated in an in vitro wound experiment. Cell culture medium obtained from the in vitro wound assay was used for biochemical analysis, and plate alcohol-fixed cells were used for immunohistochemical staining. It was determined that NPs formed an inhibition zone against the tested Gram-positive bacteria. The ZnO NPs doses determined in the MTT test provided faster wound closure in in-vitro conditions compared to the DMSO group. Biochemical analyses showed that inflammation and oxidative status decreased, while antioxidant levels increased in ZnO NPs groups. Immunohistochemical analyses showed increased expression levels of Bek/FGFR2, IGF, and TGF-β associated with wound healing. The findings reveal the antimicrobial effect of ZnO nanoparticles obtained using *Capparis spinosa* L. extract in vitro and their potential applications in wound healing.

Keywords Green Synthesis · Fibroblast Cell Line · ROS · Bek/FGFR2 · IGF · TGF-β

Responsible Editor: George Z. Kyzas

✉ Muhammed Sait Ertuğrul
sait.ertugrul@omu.edu.tr

Selma Sezen
ssezen@agri.edu.tr

Özge Balpınar
ozge.balpinar@omu.edu.tr

Cemil Bayram
cemil.bayram@atauni.edu.tr

Mustafa Özkaraca
mustafaozkaraca@cumhuriyet.edu.tr

Irmak Ferah Okkay
irmakferah@atauni.edu.tr

Ahmet Hacımüftüoğlu
ahmeth@atauni.edu.tr

Medine Güllüce
gullucem@atauni.edu.tr

[1] Department of Medical Pharmacology, Faculty of Medicine, Agri Ibrahim Cecen University, Agri, Türkiye

[2] Hemp Research Institute, Ondokuz Mayıs University, Samsun, Türkiye

[3] Department of Pharmacology and Toxicology, Faculty of Veterinary, Ataturk University, Erzurum, Türkiye

[4] Department of Pathology, Faculty of Veterinary, Sivas Cumhuriyet University, Sivas, Türkiye

[5] Department of Pharmacology, Faculty of Pharmacy, Ataturk University, Erzurum, Türkiye

[6] Department of Medical Pharmacology, Faculty of Medicine, Ataturk University, Erzurum, Türkiye

[7] Department of Biology, Faculty of Science, Ataturk University, Erzurum, Türkiye

Introduction

Wound healing is a complex process that includes hemostasis, inflammation, proliferation and tissue repair. During this process, events such as the formation of granulation tissue, contraction of the wound, proliferation of specific cells, migration, angiogenesis and re-epithelialization occur. Despite all this complex process, it is not always possible for scar tissue to be completely repaired and returned to its original state (Wang et al. 2018, Wilkinson and Hardman 2020). After injuries that may occur for various reasons, wound healing must be achieved quickly. However, aging and various diseases accompanying this process can affect wound healing and lead to chronic wound formation (Deniz 2022; Liu et al. 2022).

The formation of chronic wounds requires long-term and recurring patient care. Injuries, described as silent epidemics, affect the social and economic conditions of millions of people (Caldwell 2020). Infections associated with chronic wounds are one of the most important and common complications of skin injuries (Liu et al. 2022). Research reports that antimicrobial agents used against common infectious agents are gradually losing their effectiveness, and antimicrobial resistance has become an important problem that will affect human life in the coming years (Hassan et al. 2022; Hutchings et al. 2019; Samreen et al. 2021). Reports indicate that no new class of antibiotics has been discovered in the last 50 years, in addition, antibiotics used in different areas such as animal husbandry worsen the problem of antimicrobial resistance by exploiting the ecosystem cycle (Uddin et al. 2021; WHO 2021). In this context, there is a need to develop new low-toxicity antimicrobial agents that support wound healing (Liu et al. 2022; Wuthisuthimethawee et al. 2015). Nanotechnology has opened a new door in the development of needed therapeutic agents and regulation of drug delivery systems.

In recent years, the number of studies on hydrogels and nanoparticles and new active substances has been increasing (Baron et al. 2020; Blanco-Fernandez et al. 2021; Stan et al. 2021; Sudhasree et al. 2014). In addition to the effects of their normal chemical structures, nanoparticles can show unique effects thanks to the new characteristic structure they have acquired (Naderi et al. 2018; Yang et al. 2009). NPs are used in various fields such as diagnosis, imaging, biosensors, therapy and cosmetics. In particular, metallic NPs such as gold, silver, iron oxide, copper oxide, aluminum oxide, and zinc oxide have been proven to have antibacterial activity in association with their increased surface area/volume ratio in various previous studies (Ahmed et al. 2017; Amini 2019; Arafat et al. 2023; El-Samad et al. 2022a; Matatkova et al. 2022). NPs show their antibacterial effects through various mechanisms such as accumulation on the cell surface, interaction with the cell membrane, accumulation in the cell, damage to cellular structures such as DNA, and release of H2O2 and reactive oxygen species (ROS) (Cui et al. 2012; Lemire et al. 2013; Liew et al. 2022). In addition, ZnO NPs, which have the ability to absorb ultraviolet light, have been widely included in sunscreens, which has increased studies on the use of ZnO NPs in topical agents with different indications (Akbar et al. 2021; Rayyif et al. 2021). NPs are obtained using a variety of techniques. Conventional synthesis methods that are frequently used involve physical and chemical processes that negatively affect energy use, chemical use, and chemical release (Jamkhande et al. 2019). In addition, the formation of intermediate products that cause environmental pollution during synthesis and the insufficient pharmacokinetic findings of the NPs obtained have caused concern. Nevertheless, due to their low toxicity, environmental friendliness, and simple production steps, green synthesis techniques have drawn more attention in recent years. In the process known as green synthesis, plant metabolic products like sugars, flavonoids, terpenoids, alkaloids, phenol derivatives, and proteins are reduced with metallic ions to produce nanoparticles. The components in the biological material act as reductants and provide stabilization for the synthesis of NPs, so this method does not require the addition of external chemical stabilizers (Ahmed et al. 2017). The green synthesis method provides nanoparticles with different bioactive properties in addition to higher stability. In addition, one of the most important advantages over the conventional method is the formation of non-toxic by-products (Metwally et al. 2022; Parveen et al. 2016; Sudhasree et al. 2014).

Capparis spinosa L. (*C. spinosa* L.) (capers) (family *Capparidaceae*) is one of the wild aromatic plants commonly grown in dry regions around Central/West Asia and the Mediterranean region. Capers have been used as herbal treatment in traditional medicine for centuries due to their various properties. Aqueous extracts from the root parts of the plant have been used for their antifungal, anti-inflammatory, antidiabetic and antihyperlipidemic activities. The main flavonoids of this plant are rutin and quercetin. Rutin and quercetin are abundant in plant leaves compared to other parts of the plant. These two flavonoids are responsible for the antioxidant activity of the plant. It is thought that alkaloids such as stachydrine, cadabicine found in the roots of the plant show their antiseptic effect (Zhang and Ma 2018). Other known components are alkaloids, furan, flavonoids and pyrrole derivatives, phenolic acids, tetraterpenes, sterols, capparisine A, capparisine B, capparisine C, glucocapparin, isoginkgetin, ginkgetin, protocatechuic acid (Sezen et al. 2022). Although bioactive effects such as antimicrobial

activities, antinociceptive effects and toxicity of various NPs synthesized using different *C. spinosa* L. extracts have been investigated in previous studies, but their effects on wound healing have not been tested, to our knowledge (Benakashani et al. 2016; Mahmoudvand et al. 2020; Neamah et al. 2023).

In this study, the antimicrobial and wound healing effects of ZnO NPs synthesized using the water extract of *C. spinosa* L. fruits as a potential wound healing agent under in vitro conditions and the biological pathways of these effects were investigated.

Materials & methods

Materials

$MgSO_4.7H_2O$ (A769586 627, Purity 99.6%), KH_2PO_4 (A850773 723, purity ≥ 99.9%), and K_2HPO_4 (A851201 714, purity ≥ 98%),) were purchased from Merck, $ZnSO_4.7H_2O$ (7446–20-0, purity 99.9%), $Zn(NO_3)_2$ (228737, purity ≥ 99.9%), $ZnCl_2$ (7646–85-7, grade, ≥ 98%), $Zn(CH_3COO)_2$ (383317, grade ≥ 98%), Roswell Park Memorial Institute 1640 medium (RPMI) (R8758), Fetal Bovine Serum (FBS) (F9665), DMSO (Dimethyl sulfoxide) (D2650 grade ≥ 99.7%-D4540 grade ≥ 99.5%), and 3-(4,5-Dimethylthiazol-2-yl)-2,5-Diphenyltetrazolium Bromide (MTT) from Sigma-Aldrich, and Mueller–Hinton Agar (CM0337), Mueller–Hinton Broth (CM0337) from Oxoid.

Nanoparticle synthesis and characterization

C. spinosa L. fruits were collected from Alanya/Türkiye in August and identified (ATAHERBARIUM No 10212). After drying completely at 22 ± 4 °C, it was stored in closed containers in a cool and dark environment. While preparing the water extract, ground 20 g of *C. spinosa* L. fruits and 300 ml of distilled water were used. For nanoparticle synthesis, 1 g of the plant extract was dissolved in 5 mL of distilled water and then added slowly to 35 mL of $Zn(NO_3)_2$ solution (1 mM, pH = 8). The reaction mixture was kept on a magnetic stirrer for 6 h. After the first step of the reaction was completed, 2 M NaOH solution was added to the solution and the reaction was continued overnight at 60 °C on a magnetic stirrer. After the reaction was completed, the resulting mixture was centrifuged at 14,000 rpm for 15 min. The precipitate obtained was washed three times with alcohol and then with distilled water. After the washed precipitate was dried in the incubator at 50°C, it was ground into a fine powder with the help of a mortar and stored. Zeiss Sigma 300 and Malvern Zetasizer Nano ZSP were used to characterize the produced ZnO nanoparticles (Demir et al. 2016; Karaman et al. 2003).

Antimicrobial tests

In this study, nine standard pathogenic bacteria strains with ATCC code (Methicillin-resistant *Staphylococcus aureus* ATCC 67106, *Acinetobacter baumannii* ATCC BA1609, *Enterococcus faecium* ATCC 700211, *Escherichia coli* ATCC BAA-2523, *Streptococcus salivarius* ATCC 13419, *Pseudomonas aeruginosa* ATCC 9070, *Streptococcus mutans* ATCC 35668, *Enterococcus faecalis* ATCC 49452, *Bacillus cereus* ATCC 14579) taken from the bacterial collection of Atatürk University Biology Department Bacteriology Laboratory were used. To determine antimicrobial activity, 12-h bacterial suspensions inoculated in Mueller–Hinton Broth medium were adjusted to 0.5 McFarland standard turbidity. ZnO NPs were applied at a dose of 10 µg/mL using the agar well diffusion methods. The antibacterial effect was determined by measuring the inhibition zone around the wells after 12 h of incubation at 37°C (Klink et al. 2022).

Cell culture dose studies

Fibroblast cell lines obtained from Atatürk University Faculty of Medicine, Department of Medical Pharmacology were grown in flasks in RPMI medium containing 10% FBS/1% Antibiotic. After the flask surfaces were completely covered, the obtained cells were seeded in 96-well plates at 5000–6000 cells per well. The cells in the well were treated with the nanoparticle doses (0.0390625 µg/mL, 0.078125 µg/mL, 0.15625 µg/mL, 0.3125 µg/mL, 0.625 µg/mL, 1.25 µg/mL, 2.5 µg/mL, 5 µg/mL, 10 µg/mL, and 20 µg/mL) obtained after covering approximately 80% of the well surface. Cell viability was evaluated by adding 5 mg/ml MTT solution to the cells exposed to nanoparticles for 24 h (Ertugrul et al. 2020).

In vitro Scratch wound healing assay

For cell migration measurement, cells grown in RPMI medium containing 10% FBS / 1% antibiotic were seeded in 24-well plates. When the seeded cells completely covered the surface of the well, they were scratched thoroughly with a 100 µL pipette tip. The plate was washed with PBS solution to prevent the floating cells from re-adhering to the scratched area. The nanoparticle doses determined as a result of the MTT test were added to the wells. Cells were photographed with Leica DFC 295 inverted microscope every 12 h and the wound closure areas were calculated with the help of the ImageJ program using the photographs in all groups (Addis et al. 2020).

Biochemical analyzes

TAC (Total Antioxidant Capacity)/TOS (Total Oxidant Status) kits from Rel Assay Diagnostic and Interleukin 6 (IL-6) and Tumor necrosis factor-alpha (TNF-α) kits from Elabscience were used for biochemical analysis following kit procedures. For TAC kit; 18 µL of sample samples and standards were taken and added to the wells. After adding 300 µL of Reagent 1 to these, the Heidolph Microtiter Plate Shaker is held in Titramax at 300 rpm for 30 s to thoroughly mix the well contents. The first reading was taken at 660 nm. After the first reading, 45 µL of Reagent 2 was added to all wells and kept in the shaker again to ensure a homogeneous mixture. After this process, it was left to incubate at 37 °C for 5 min. At the end of the incubation process, absorbance is read again at 660 nm. Results were calculated according to the formula in the kit procedure. For TOS kit; 45 µL of sample and standard were taken and added to the wells. After adding 300 µL of Reagent 1 to these, the Heidolph Microtiter Plate Shaker was held in Titramax at 300 rpm for 30 s to thoroughly mix the well contents. The first reading was taken at 530 nm. After the first reading, 15 µL of Reagent 2 was added to all wells and kept in the shaker again to ensure homogeneous mixing. After this process, it was left to incubate at 37 °C for 5 min. At the end of the incubation process, absorbance was read again at 530 nm. The results were calculated according to the formula in the kit procedure (Taghizadehghalehjoughi et al. 2019).

For TNF-α and IL-6; 100 µL of sample and standard were added to the plate wells. The plate was then incubated at 37 °C for 90 min. At the end of the incubation period, the liquid in the plate was completely emptied and the Biotinylated Detection Ab working solution was added to the wells. After this process, it was incubated again at 37 °C for 60 min. At the end of the incubation period, the plate was aspirated and washed three times with washing solution. 100 µL of HRP conjugate working solution was added to the washed wells and incubated at 37 °C for 30 min. At the end of the incubation period, the washing process was repeated five more times. Then, 90 µL of substrate reagent was added to the wells and incubated for another 15 min at 37 °C. Finally, 50 µL of stop solution was added and the plate was read at 450 nm (Ferah Okkay et al. 2022; Kesmez Can et al. 2021).

Immunohistochemistry staining

After the Scratch Wound Healing Assay, 24-well plates were fixed with cold methanol for 5 min at -20ºC. After fixation, the methanol in the 24-well plate was poured and washed with PBS. It was then incubated for 15 min in PBS solution containing 0.1% Triton X-100 at 22 ± 4 °C. At the end of the waiting period, the plate was washed with PBS. After washing, it was incubated in a PBS solution containing 2% BSA for 60 min at 22 ± 4 °C. The washing process was repeated. Then monoclonal anti-Bek/FGFR2 (Fibroblast Growth Factor Receptor 2) (Santa Cruz, Catalog no. sc-6930), monoclonal anti-IGF (Insulin-Like Growth Factor) (Santa Cruz, Catalog no. sc-518040) and monoclonal anti-TGF-β (Transforming Growth Factor Beta) (Santa Cruz, Catalog no. sc-130348) primers were incubated overnight at + 4ºC at a dilution rate of 1/200 with antibodies. After the incubation, the washing process was repeated and the washed cells were incubated in the dark at 22 ± 4 °C for 1 h with goat anti-mouse FITC secondary antibody at a dilution ratio of 1/100, in accordance with the primary antibodies used. After washing, 4′,6-diamidino-2-phenylindole (DAPI) was dropped on the cells and examined under a fluorescence microscope. Fluorescence positivity seen near the wound line was evaluated semi-quantitatively as absent (-), mild (+), moderate (++), and severe (+++) (Sezen et al. 2023).

Statistical analysis

Data from MTT, TAC, TOS, TNF-α, IL-6, and immunohistochemistry were analyzed with the SPSS 20.00 program. The difference between the groups in immunohistochemistry findings was determined by Kruskal Wallis, one of the nonparametric tests, and the group that created the difference was determined by the Mann–Whitney U test ($p < 0.05$, $p < 0.001$). One-Way Anova, one of the parametric tests, was used for other analyses ($p < 0.05$, $p < 0.001$) (Taghizadehghalehjoughi et al. 2020).

Results

Nanoparticle synthesis

Zetasizer is a system that measures particle size with the dynamic light scattering (DLS) method, also known as Photon correlation spectroscopy (PCS). The basic principle of measurement is Brownian movements. Brownian movements of the suspended material cause the laser light to be scattered at different intensities. In analyzing these density fluctuations, particle size is calculated using the Stokes–Einstein relationship (Inam and Peijs 2006).

A scanning electron microscope (SEM) is an imaging system that uses electrons instead of a light source to create images. The electron beam follows a linear path under vacuum, passing through electromagnetic fields and lenses. When the beam hits the sample, it disperses, scattering secondary electron beams and X-rays. Images are obtained with the help of these rays collected by detectors (Akhtar et al. 2018).

When the ZnO nanoparticles synthesized through green synthesis with *C. Spinosa* were examined with the Zetasizer,

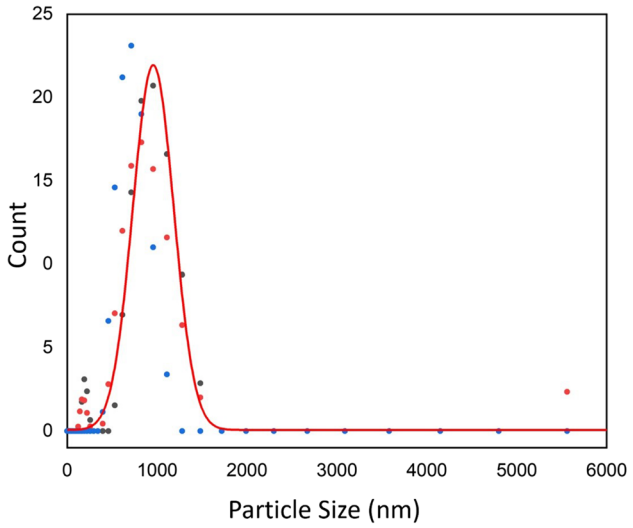

Fig. 1 Green synthesized ZnO nanoparticle Zetasizer results

it was observed that the particle size distribution reached 6 µm. The average particle size was 1000 nm (Fig. 1). The data obtained from the Zetasizer overlaps to a certain extent with the SEM images (Fig. 2A).

In the analysis of SEM images of nanoparticles, it was observed that the particles were irregular at 2.00 KX magnification (Fig. 2A). However, when examined at magnifications of 50.00 KX and higher, it was determined that the irregular particles consisted of nanorods (Fig. 2B). When examined with 150.00 KX, it was determined that these nanorods were 300–400 nm in length and 60–100 nm in diameter. It was also determined that these nanorods grew adherent to each other (Fig. 2C). When the nanorods were examined at a magnification of 200.00 KX, it was observed that they consisted of grains smaller than 10 nm (Fig. 2D).

When the Zetasizer and SEM images were examined, the structure of the obtained material was clarified. It has been determined that the developed material has nanoparticle properties.

Antimicrobial

ZnO NPs showed varying antimicrobial activity against standard pathogenic bacterial strains. When evaluated according to Gram characteristics, while inhibition zone was formed in Gram-positive bacteria strains, no inhibition zone was detected against Gram-negative bacteria. Antimicrobial zone diameters

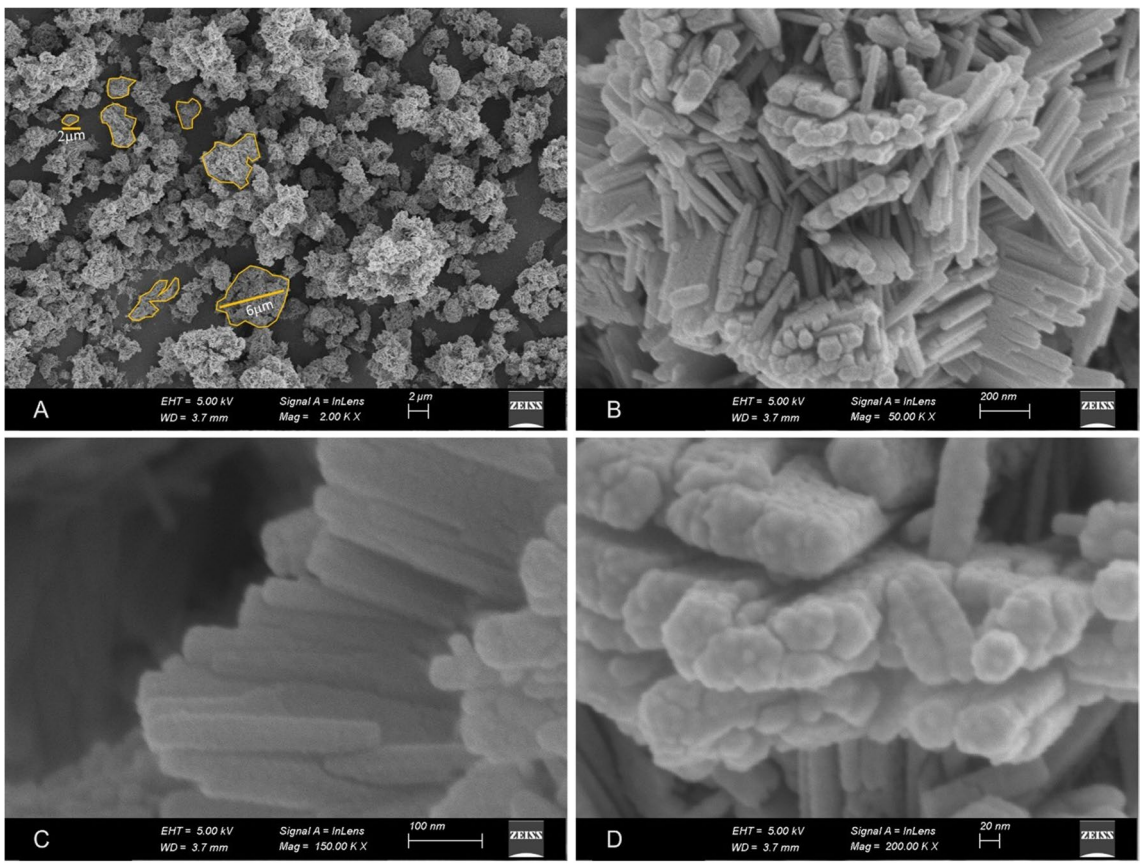

Fig. 2 Green synthesized ZnO nanoparticle SEM image

against pathogens were determined as Methicillin-resistant *Staphylococcus aureus* ATCC 67106 (5 mm), *Enterococcus faecium* ATCC 700211 (8 mm), *Streptococcus mutans* ATCC 35668 (9 mm), *Streptococcus salivarius* ATCC 13419 (8 mm).

MTT

MTT assay was performed to determine the effect of different doses (0.0390625 µg/mL, 0.078125 µg/mL, 0.15625 µg/mL, 0.3125 µg/mL, 0.625 µg/mL, 1.25 µg/mL, 2.5 µg/mL, 5 µg/mL, 10 µg/mL, and 20 µg/mL) of ZnO NPs on cell viability. When the data obtained from the MTT test were analyzed, it was observed that cell viability increased significantly increase in the 0.15625 µg/mL, 0.3125 µg/mL, 0.625 µg/mL, and 1.25 µg/mL dose groups compared to the Control ($p < 0.05$). In addition, it was observed that NPs had a toxic effect after a dose of 2.5 µg/mL (Fig. 3). In the MTT assay, the proliferative doses of ZnO NPs were determined as 0.0390625 µg/mL, 0.078125 µg/mL, 0.15625 µg/mL, 0.3125 µg/mL, 0.625 µg/mL, 1.25 µg/mL and these doses were used for the scratch wound healing assay.

Scratch wound healing assay

The proliferative doses determined as a result of the MTT test were applied to the plate after creating straight lines on the fibroblast cells planted on 24-well plates. When the images obtained with the inverted microscope were examined with the ImageJ program, cell bridges began to form in the Control group from the 24th hour, and complete wound closure was observed in this group at the 48th hour. In the DMSO group, cell bridges and wound closure did not occur until the 48th hour. When the treatment groups were examined, it was determined that cell bridges were formed starting from the 36th hour and the wound line was closed significantly by the 48th hour. When the wound area calculations of the experimental groups were examined, it was determined that proliferation and migration were at the highest level at the doses of 0.625 µg/mL and 1.25 µg/mL ($p < 0.001$) (Figs. 4, and 5).

Biochemical analyzes

IL-6 and TNF-α levels, which are important inflammation markers in wound healing, were determined at the media obtained as a result of the scratch wound healing assay. IL-6 level increased in DMSO, 0.0390625 µg/mL, 0.078125 µg/mL, 0.15625 µg/mL, and 0.3125 µg/mL doses compared to the Control group. IL-6 levels were found to be close to the Control group at the doses of 0.625 µg/mL and 1.25 µg/mL, where wound closure was greater. Statistically, a significant difference was determined only in the DMSO group. When TNF-α levels were examined, it was

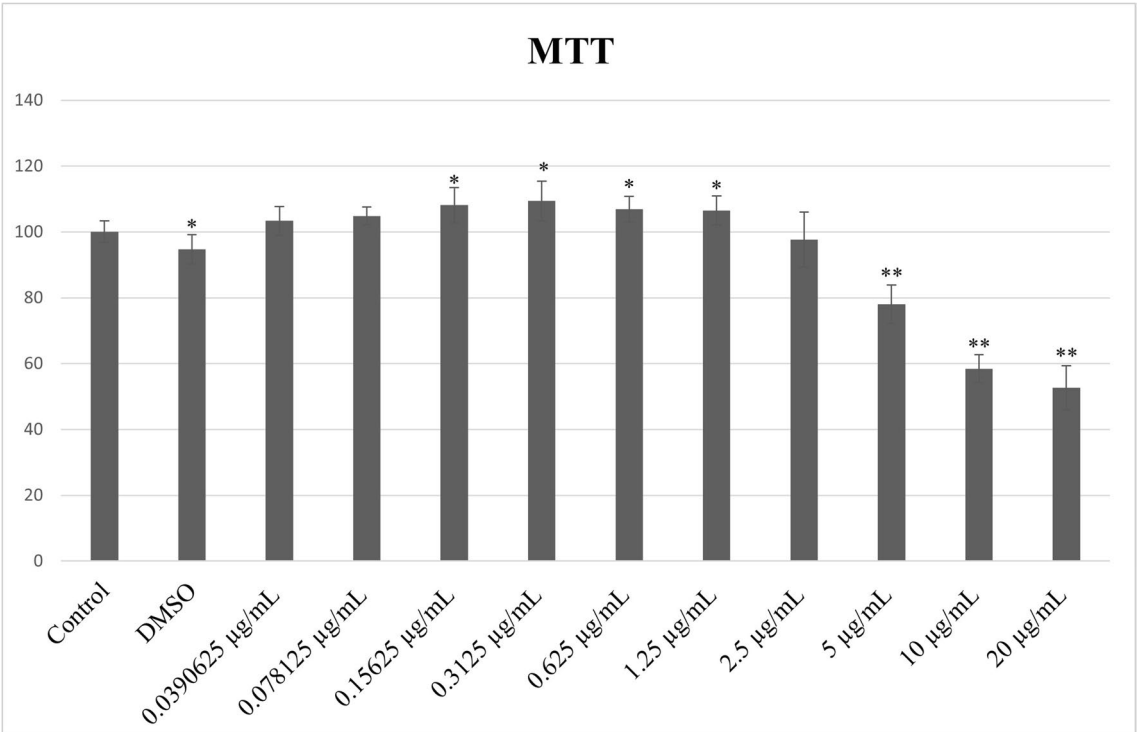

Fig. 3 Cell viability measurement results with MTT ($p < 0.05$, the difference between groups *; $p < 0.001$, the difference between groups **)

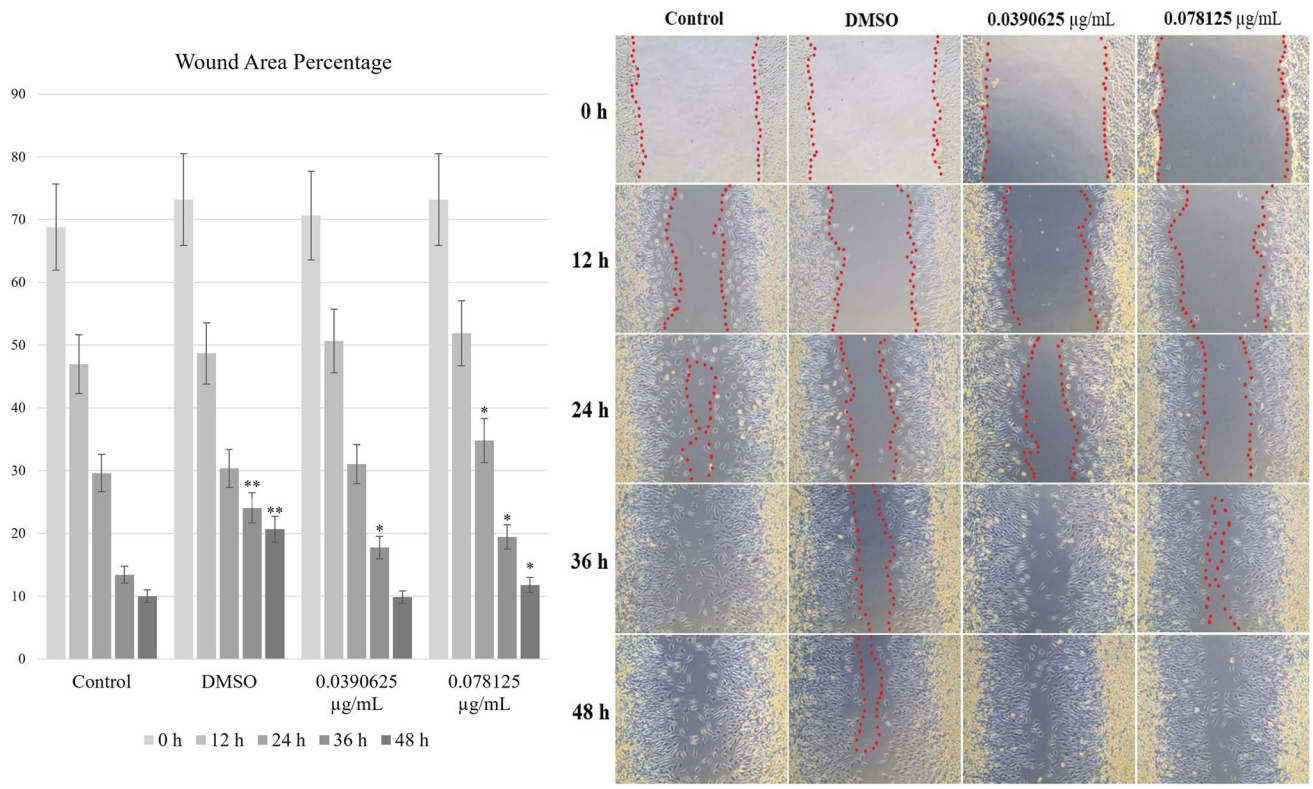

Fig. 4 Scratch Wound Healing Assay Control, DMSO, 0.0390625 µg/mL, 0.078125 µg/mL ($p < 0.05$, the difference between groups *; $p < 0.001$, the difference between groups **)

observed that all doses were lower than the DMSO group. There was no statistically significant difference between the groups. However, TNF-α level was lower than both the Control and DMSO groups at the dose of 1.25 µg/mL, which is one of the groups with high wound closure (Fig. 6).

Considering the oxidant status data, it was seen that the DMSO group increased the TOS level excessively, and this level decreased as the dose increased, depending on the dose of the applied nanoparticle. In the scratch wound healing assay, the treatment doses with the lowest oxidative levels were determined as 0.3125 µg/mL, 0.625 µg/mL, and 1.25 µg/mL. When the effects of doses on total antioxidant capacity were examined, it was determined that antioxidant capacity generally increased significantly at 0.15625 µg/mL, 0.3125 µg/mL, 0.625 µg/mL, and 1.25 µg/mL doses ($p < 0.05$, $p < 0.001$). When total oxidant status and total antioxidant capacities are compared, it is seen that these data are correlated to support each other (Fig. 7).

Immunohistochemistry

Bek/FGFR2, IGF and TGF-β levels, which are important parameters in wound healing, were examined immunohistochemically. In Bek/FGFR2 fluorescence staining results, mild immunopositivity was observed in the groups between the Control and 0.15625 µg/mL. It was determined that immunopositivity increased to a moderate level at doses of 0.3125 µg/mL, 0.625 µg/mL, and 1.25 µg/mL. In the IGF staining results, while significant positivity was not observed in the Control and DMSO groups, mild positivity was observed in the groups between 0.0390625—0.3125 µg/mL doses, and severe positivity was observed in the 0.625 µg/mL, and 1.25 µg/mL groups. When TGF-β staining was examined, moderate positivity was observed in the 0.625 µg/mL group, and severe positivity was observed in the 1.25 µg/mL group, while mild positivity was observed in the other groups. (Table 1, Figs. 8, 9, and 10).

Discussion

Acute and chronic injuries cause significant health expenditures even in developing countries. The desired condition in the treatment processes of injuries is rapid wound healing and re-epithelialization (Vijayakumar et al. 2019). However, the healing processes in chronic injuries are prolonged as a result of events such as chronic inflammation,

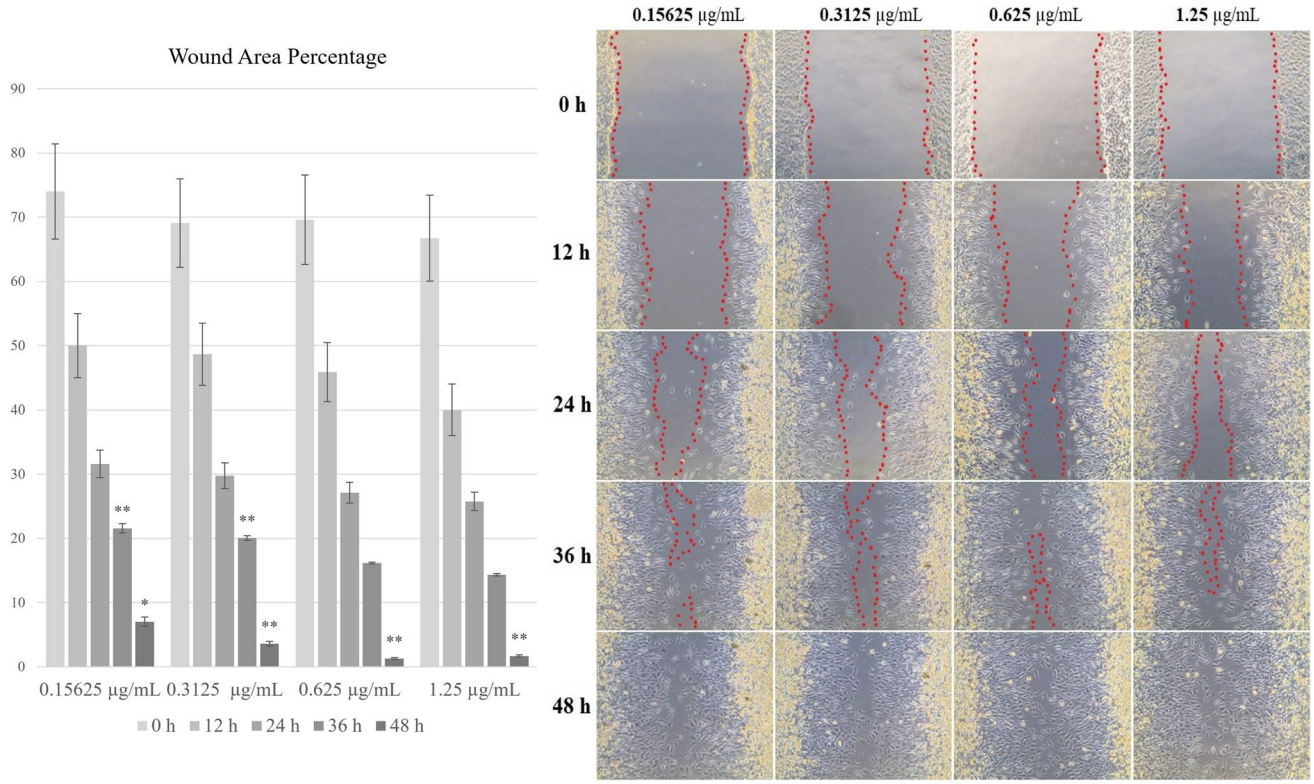

Fig. 5 Scratch Wound Healing Assay 0.15625 µg/mL, 0.3125 µg/mL, 0.625 µg/mL, 1.25 µg/mL ($p < 0.05$, the difference between groups *; $p < 0.001$, the difference between groups **)

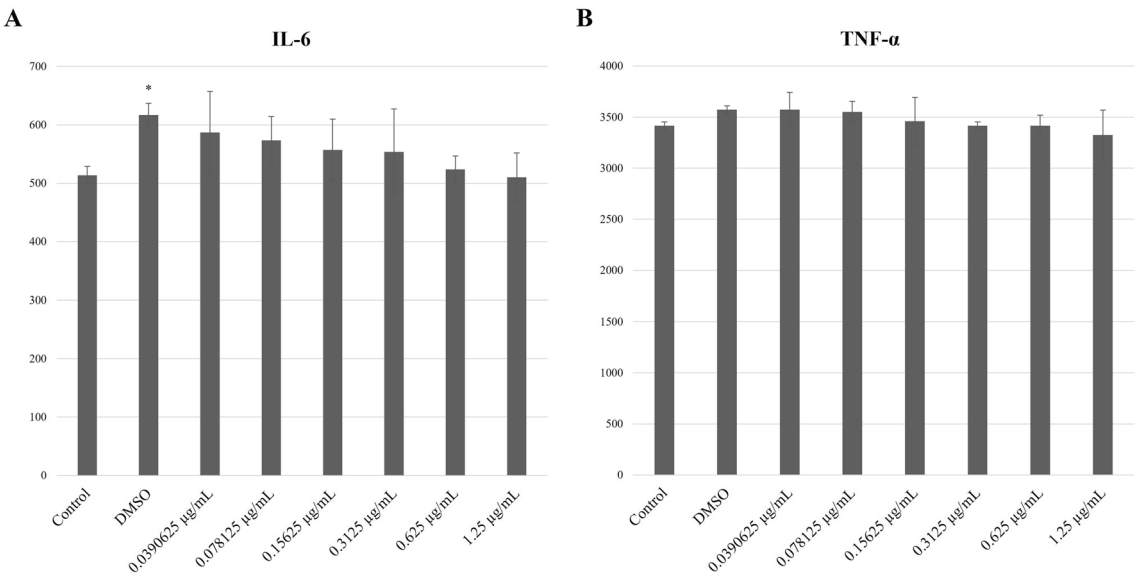

Fig. 6 IL-6 and TNF-α results (*$p < 0.05$, the difference between groups, **$p < 0.001$, the difference between groups)

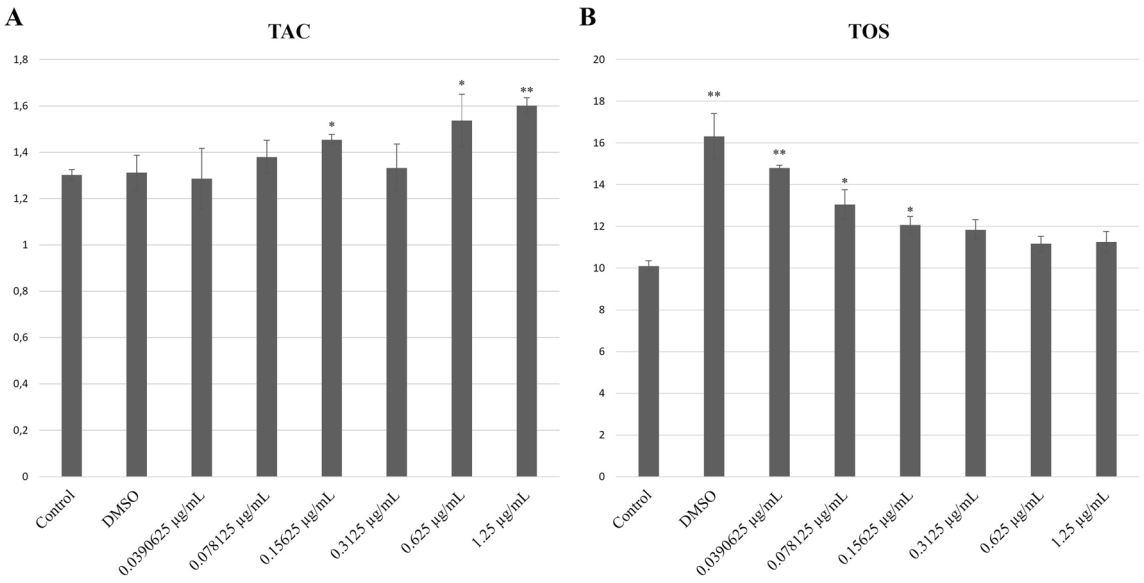

Fig. 7 TAC and TOS results ($p < 0.05$, the difference between groups *; $p < 0.001$, the difference between groups **)

Table 1 Statistical differences in Bek/FGFR2, IGF and TGF-β immunofluorescence staining. ($p < 0.001$, the difference between groups ^{a,b,c})

Groups	Bek/FGFR2	IGF	TGF-β
Control	0.83 ± 0.40^{a}	0.33 ± 0.40^{a}	1.00 ± 0.00^{a}
DMSO	1.00 ± 0.00^{a}	0.33 ± 0.40^{a}	1.16 ± 0.40^{a}
0.0390625 µg/mL	1.00 ± 0.00^{a}	0.83 ± 0.00^{b}	1.00 ± 0.00^{a}
0.078125 µg/mL	1.16 ± 0.40^{a}	0.83 ± 0.40^{b}	1.16 ± 0.40^{a}
0.15625 µg/mL	1.16 ± 0.40^{a}	1.00 ± 0.00^{b}	1.00 ± 0.00^{a}
0.3125 µg/mL	2.00 ± 0.40^{b}	1.16 ± 0.40^{b}	1.00 ± 0.00^{a}
0.625 µg/mL	1.83 ± 0.40^{b}	2.66 ± 0.51^{c}	2.00 ± 0.00^{b}
1.25 µg/mL	1.83 ± 0.40^{b}	2.83 ± 0.40^{c}	2.66 ± 0.51^{c}

increased ROS amount and increased neutrophil infiltration. Wound infection, which is one of the most important factors in the chronicity of wounds, is a frequently encountered problem (Gao et al. 2017; Liu et al. 2022). The development of resistance to antibiotics used to treat of infections has pushed the scientific world to search for different treatment options. In the last quarter century, nanoparticles have been widely investigated in all treatment approaches, as well as in acute and chronic wound treatment (Stan et al. 2021; Vijayakumar et al. 2019; Wang et al. 2018).

The main flavonoids of the *C. spinosa* L. plant, which is used as an antiseptic agent in Iran, are rutin and quercetin. The antioxidant property resulting from the using the plant extract is related to these two flavonoids. It is thought that alkaloids such as stachhydrin, cadabicine found in the roots of the plant have an antiseptic effect (Zhang and Ma 2018). Other known components are alkaloids, furan, flavonoids and pyrrole derivatives, phenolic acids, tetraterpenes, sterols, capparisine A, capparisine B, capparisine C, glucocapparin, isoginkgetin, ginkgetin, protocatechuic acid (Sezen et al. 2022).

Zinc is an essential element in many metabolic events such as growth, development, immunity, and wound healing. These ions exert their effects on immunity by acting on the regulation of chemokines and cytokines through platelets (Lin et al. 2017). It supports its effects on wound healing by increasing platelet activity and providing coagulation. ZnO nanoparticles, which are based on Zn as a metallic ion, show antibacterial and anticancer activity. It provides these effects mainly by increasing ROS levels, maintaining the tumor suppressor p53 gene activity and activating the caspase-6 enzyme. There are studies showing that, in addition to ROS production, ultraviolet light induction, Zn ion release and other physicochemical properties play a role in the antimicrobial effect of ZnO NPs (Akbar et al. 2021, Aslam et al. 2022, Gharpure and Ankamwar 2020, Kaushik et al. 2019, Lin et al. 2017, Sharma et al. 2012). In addition, ZnO NPs have high adhesion to the bacterial cell membrane (Gao et al. 2017).

There are many wound healing studies with ZnO nanoparticles depending on their antimicrobial activity. In these studies, it has been shown that the effects of nanoparticles on inflammatory processes affect the wound healing process (Harandi et al. 2021; Lin et al. 2017). In addition, in a study with hydrogels using ZnO NPs, it was shown that ZnO NPs inhibited biofilm formation (Rayyif et al. 2021). According to the results obtained in this study with ZnO NPs, antimicrobial activity was observed in Gram-positive

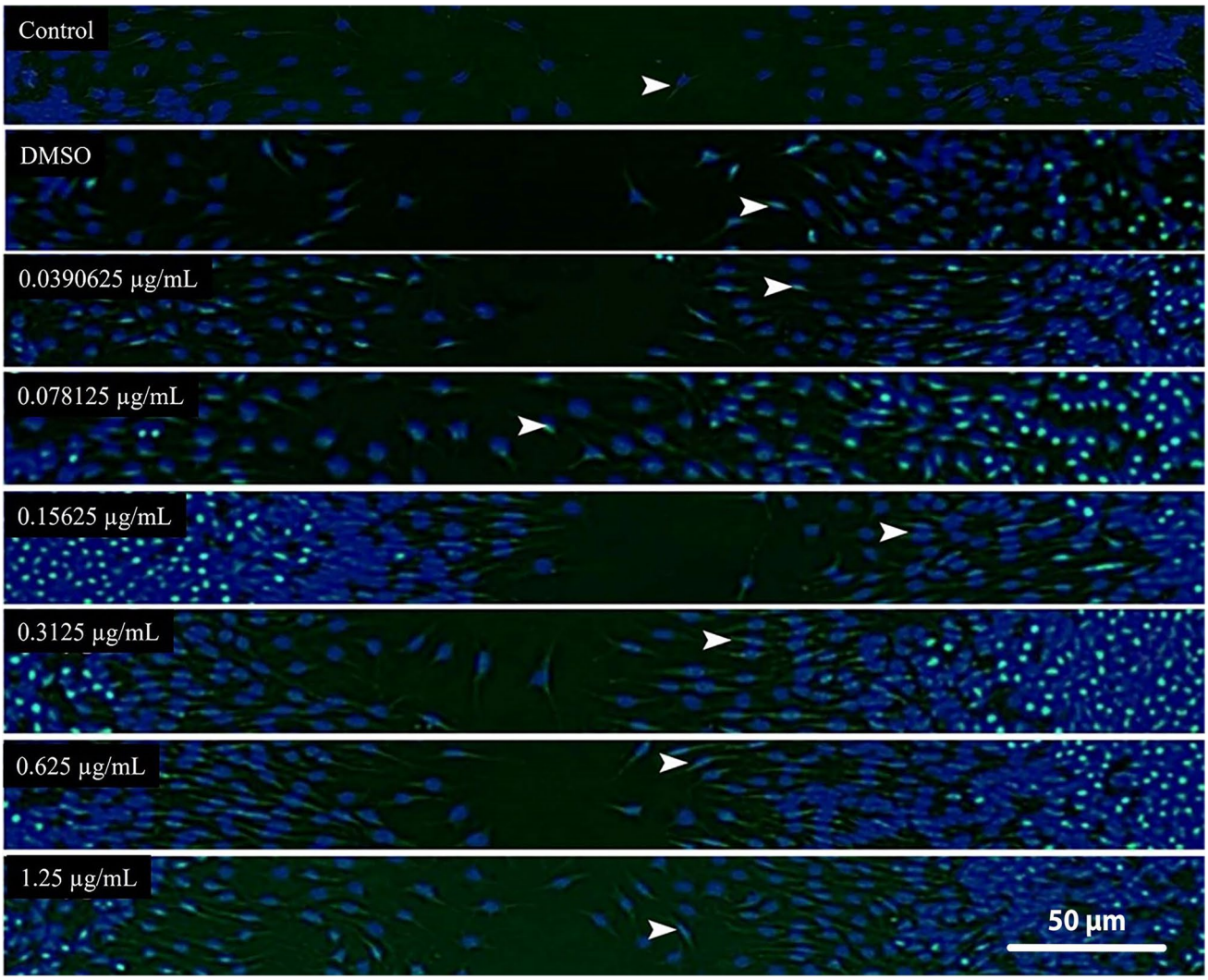

Fig. 8 Bek/FGFR2 immunofluorescence staining. Mild expression (arrowhead) in the Control, DMSO, 0.0390625 µg/mL. 0.078125 µg/mL, and 0.15625 µg/mL groups and moderate expression in the 0.3125 µg/mL. 0.625 µg/mL and 1.25 µg/mL groups

strains tested. In a study on fibroblast cells, it was seen that it supports fibroblast adhesion and migration. It is emphasized in the literature that collagen accumulation occurs in the wound area as a result of migration. It is reported that this situation accelerates the wound healing process (Yang et al. 2009). They determined that the carboxymethyl cellulose/sericin-based hydrogel developed by El-Samad et al. created a strong inhibition zone against five multidrug-resistant strains. In addition, although the hydrogel had a strong antimicrobial effect, it reduced oxidative stress in the skin tissue of diabetic rats (El-Samad et al. 2022b). the results obtained were examined, it was observed that ZnO NPs obtained from *C. spinosa* L. plant extract showed antimicrobial activity on Methicillin-resistant *Staphylococcus aureus* ATCC 67106, *Enterococcus faecium* ATCC 700211, *Streptococcus mutans* ATCC 35668, *Streptococcus salivarius* ATCC 13419 lines. It has been proven in the literature that ZnO NPs can exert an antibacterial effect by forming H_2O_2 (Kaushik et al. 2019). When other data obtained are examined, it is thought that this antimicrobial effect is not only due to reactive oxygen. Because, according to the TOS and TAC analyses, it was observed that there was no increase in reactive oxygen species. Neamah et al. reported that the ZnO NPs they synthesized using the water extract of *C. spinosa* L. fruit exhibited strong antioxidant activity in the DPPH test at doses of 7.5–300 µg/mL (Neamah et al. 2023). In another literature, it has been shown that ZnO NPs can cause cellular damage by affecting cell integrity by showing adhesion to the cell membrane through electrostatic interactions (Gao et al. 2017; Hassan et al. 2023). It is thought that the antibacterial effect obtained is through this pathway.

As a result of MTT analysis, it is observed that cell viability increases up to 1.25 µg/mL and starts to decrease at higher doses. It is observed that cell viability decreases

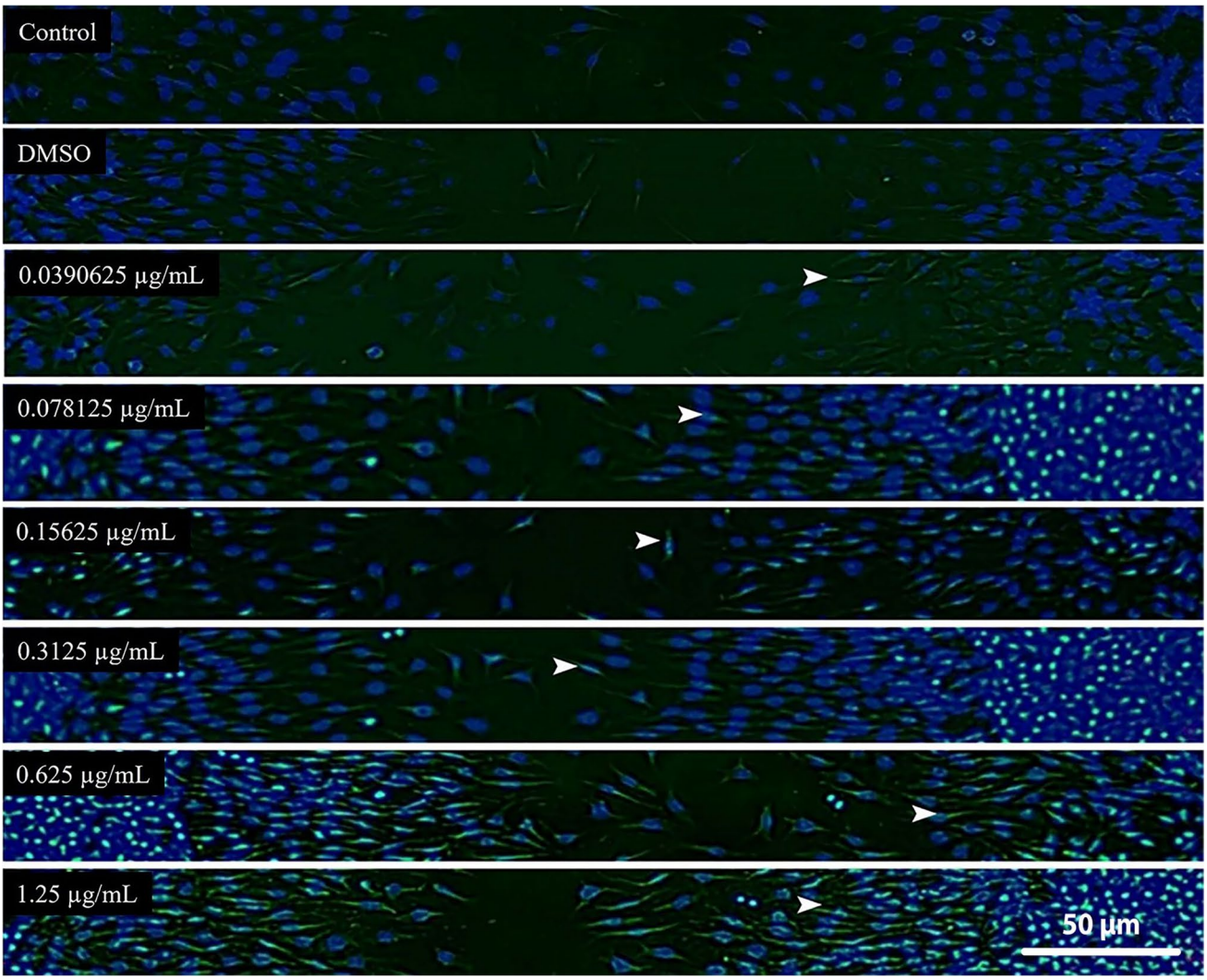

Fig. 9 IGF immunofluorescence staining. Negativity in the Control and DMSO groups mild expression (arrowhead) in the 0.0390625 µg/mL, 0.078125 µg/mL, 0.15625 µg/mL and 0.3125 µg/mL groups and severe expression in the 0.625 µg/mL and 1.25 µg/mL groups

significantly at 5–10-20 µg/mL doses ($p < 0.001$). Zinc has effects on regulatory T lymphocytes (Treg). Increased Treg levels with zinc supplementation result in the resolution of inflammation and TGF-β-mediated re-epithelialization. Zinc also takes part in the formation of granulation tissue (Lin et al. 2017). It can be thought that the severe decrease in cell viability at doses of 5–20 µg/mL may be mediated by a possible toxic effect due to increased phenolic substance concentration and/or by the mechanisms mentioned in the antibacterial activity caused by Zn^{+2} ions. Zn^{+2} ions affect the wound healing process by increasing platelet activity and providing coagulation (Mammadova-Bach and Braun 2019). In addition, it can be thought that ZnO NPs increase cell division by increasing cellular migration and collagen deposition at the wound site (Metwally et al. 2022). As a result of the data obtained from the MTT result of the study, when the selected doses were applied in the cell migration assay, it was observed that the wound areas formed were closed in a way correlated to the MTT results.

When IL-6 and TNF-α levels were examined after the scratch wound healing test, it was observed that IL-6 and TNF-α levels decreased with increasing doses. As is known, ZnO NPs have anti-inflammatory effects on inflammatory cytokines. The decrease in IL-6 and TNF-a levels may be due to these effects of ZnO NPs. However, it can be thought that ZnO NPs activities on p53 gene and caspases may also affect inflammatory factors through the mechanism of repair of DNA damage (Sharma et al. 2012). In the obtained data, it is seen that TAC and TOS levels were correlated with each other. With increasing doses, a decrease in oxidant status and an increase in antioxidant capacity were observed. Studies in the literature have shown that ZnO NPs have an oxidant effect by producing H_2O_2 (Elshama et al. 2018). However, in contrast to this situation, oxidant status decreased, and

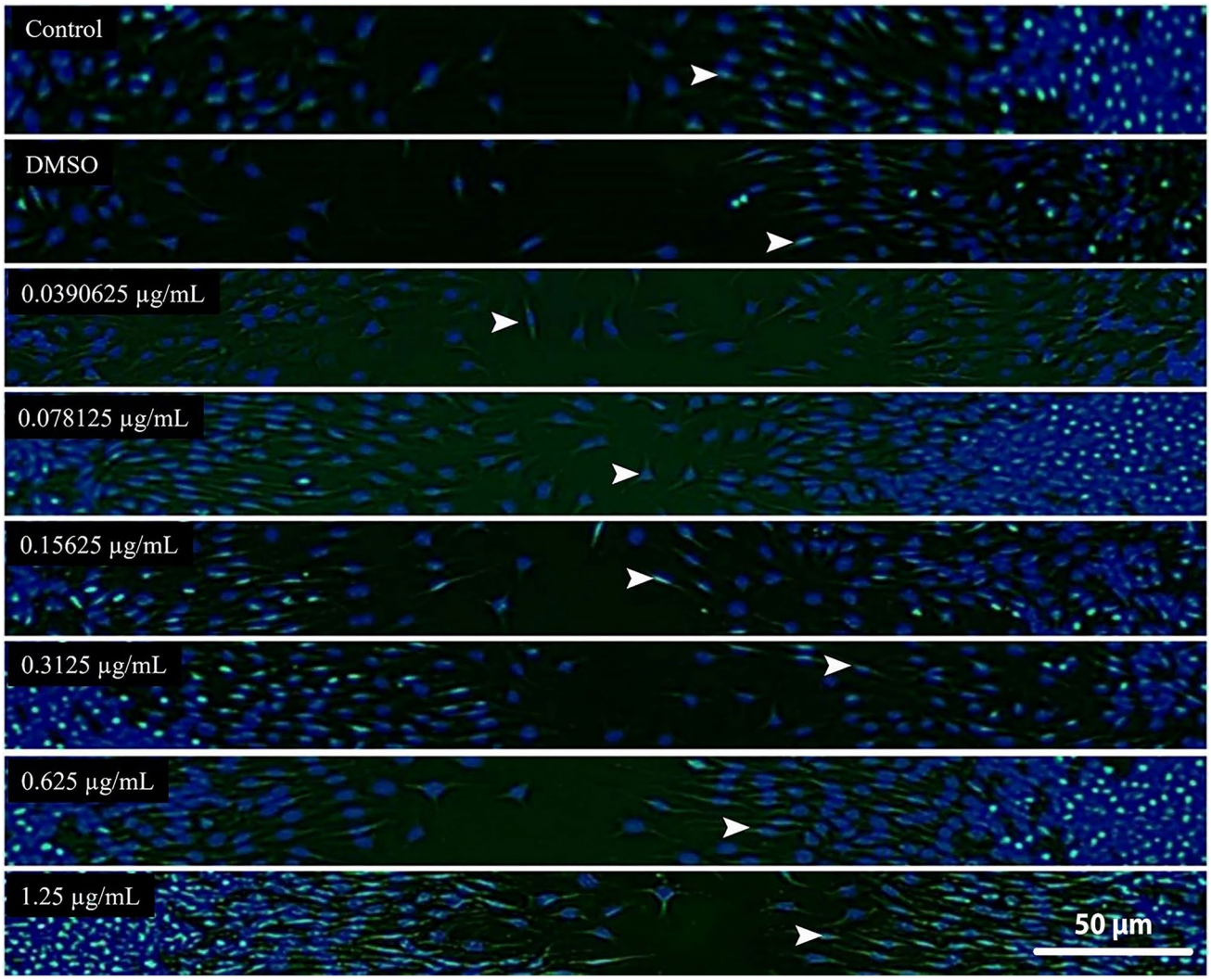

Fig. 10 TGF-β immunofluorescence staining. Mild expression (arrowhead) in the Control, DMSO, 0.0390625 µg/mL, 0.078125 µg/mL, 0.15625 µg/mL, and 0.3125 µg/mL groups moderate expression in the 0.625 µg/mL group, and severe expression in the 1.25 µg/mL group

antioxidant capacity increased with increasing doses. The reason for this may be that the stability of ZnO NPs obtained by green synthesis is higher than that of chemically obtained zinc NPs (Metwally et al. 2022; Parveen et al. 2016; Sudhasree et al. 2014). It may have prevented the steady-state Zn^{+2} ions from being released enough to increase oxidative stress. In addition, zinc deficiency and excess inhibit NADPH oxidase, which is important for the formation of ROS precursors. The decrease in oxidant status at the determined doses can be thought to be mediated by the inhibition of NADPH oxidase dependent on the amount of zinc (Lin et al. 2017).

Bek/FGFR2 is a member of the fibroblast growth factor family (Liu et al. 2021). It is one of the cell signaling proteins produced by macrophage cells. It is involved in wound healing and regulation of hepatic stellate cells (Dolivo et al. 2017; Liu et al. 2021). As is known, zinc plays a role in the differentiation of monocytes into macrophages (Lin et al. 2017). There is also evidence showing that it increases keratinocyte motility and migration of fibroblasts (Sogabe et al. 2006). In the scratch wound healing test performed, it was determined that Bek/FGFR2 immunopositivity was higher in the groups treated with 0.3125 µg/mL, 0.625 µg/mL, and 1.25 µg/mL doses with high proliferation and migration compared to the other groups. It can be said that the increase in BEK levels depending on the dose increase is due to the differentiating effect of zinc ions on cells. Another important parameter in wound healing is TGF-β level. TGF-β is also involved in the regulation of the extracellular matrix. In the literature, data showing that the increase in TGF-β and Bek/FGFR2 levels are parallel is presented (Kanda et al. 2003; Penn et al. 2012). When the TGF-β data were analyzed, the results showed a significant increase in the doses of 0.625 µg/mL and 1.25 µg/mL compared to the Control. The effect of increasing doses of zinc ions on cell

proliferation was proven by the increase in TGF-β levels, and at the same time, the relationship between TGF-β and Bek/FGFR2 levels was confirmed. Another important factor is IGF. It is involved in the proliferation of fibroblast cells and the stimulation of cellular migration. Their expression in injured tissues is considerably higher than in healthy tissues (Hadley et al. 2010; Roberts et al. 2022). It was observed that IGF levels increased significantly in all dose groups compared to the Control, and this significance was even stronger at 0.625 µg/mL and 1.25 µg/mL doses. The proliferative effect of ZnO NPs and the tumor suppressor p53 gene mediated DNA repair mechanisms may have caused an increase in TGF-β, IGF and Bek/FGFR2 levels.

Conclusion

Although nanotechnology has applications in many spheres of life, it has offered new possibilities and methods, particularly in the field of medical technologies. As an important public health problem, it was determined that ZnO NPs produced by green synthesis using *Capparis spinosa* L. water extract, which we discussed in this study in terms of antimicrobial agents and wound healing, had an average size of 1000 nm. It was confirmed that ZnO NPs showed antimicrobial effects against four strains among nine different pathogenic bacteria. In studies testing the viability and proliferation of human fibroblast cells, it was observed that ZnO NPs increased cell viability up to a dose of 1.25 µg/mL and caused a decrease in cell viability at doses above this. In the in vitro wound healing study, where a safe dose range was used, it was determined that all treatment doses provided faster wound closure than the DMSO group. These results showed that the synthesized ZnO NPs have the potential to be used in the development of topical formulations and various biomedical materials that will accelerate wound healing. However, comprehensive in vivo studies are needed for this green synthesis product ZnO NPs with important bioactive properties.

Acknowledgements Thank to for the taxonomic identification Prof. Dr. Meryem Sengul Koseoglu.

Author contribution Selma Sezen: Investigation, Conceptualization, Original draft, Writing-review & editing
Muhammed Sait Ertugrul: Data Curation, Methodology
Ozge Balpinar: Original draft, Writing-review & editing
Cemil Bayram: Formal analysis, Writing-review & editing
Mustafa Ozkaraca: Methodology, Formal analysis
Irmak Ferah Okkay: Methodology, Formal analysis
Ahmet Hacimuftuoglu: Resources, Supervision & editing
Medine Gulluce: Resources, Supervision & editing

Funding The authors declare that no funds, grants, or other support were received during the preparation of this manuscript.

Data availability This publication's research data and supporting information are available here and mentioned in the manuscript.

Declarations

Ethical approval Not applicable.

Consent to participate Not applicable.

Consent to publish Not applicable.

Conflict of interest The authors declare that we do not have any commercial or associative interest that represents a conflict of interest in connection with the work submitted.

References

Addis R, Cruciani S, Santaniello S, Bellu E, Sarais G, Ventura C, Maioli M, Pintore G (2020) Fibroblast Proliferation and Migration in Wound Healing by Phytochemicals: Evidence for a Novel Synergic Outcome. Int J Med Sci 17:1030–1042. https://doi.org/10.7150/ijms.43986

Ahmed S, Annu CSA, Ikram S (2017) A review on biogenic synthesis of ZnO nanoparticles using plant extracts and microbes: A prospect towards green chemistry. J Photochem Photobiol B 166:272–284. https://doi.org/10.1016/j.jphotobiol.2016.12.011

Akbar N, Aslam Z, Siddiqui R, Shah MR, Khan NA (2021) Zinc oxide nanoparticles conjugated with clinically-approved medicines as potential antibacterial molecules. Amb Express 11:104. https://doi.org/10.1186/s13568-021-01261-1

Akhtar K, Khan SA, Khan SB, Asiri AM (2018) Scanning electron microscopy: Principle and applications in nanomaterials characterization. Handbook of materials characterization: 113–145 https://doi.org/10.1007/978-3-319-92955-2_4

Amini SM (2019) Preparation of antimicrobial metallic nanoparticles with bioactive compounds. Mater Sci Eng C Mater Biol Appl 103:109809. https://doi.org/10.1016/j.msec.2019.109809

Arafat EA, El-Sayed DS, Hussein HK, Flaven-Pouchon J, Moussian B, El-Samad LM, El Wakil A, Hassan MA (2023) Entomotherapeutic Role of Periplaneta americana Extract in Alleviating Aluminum Oxide Nanoparticles-Induced Testicular Oxidative Impairment in Migratory Locusts (Locusta migratoria) as an Ecotoxicological Model. Antioxidants (Basel) 12. https://doi.org/10.3390/antiox12030653

Aslam Z, Roome T, Razzak A, Aslam SM, Zaidi MB, Kanwal T, Sikandar B, Bertino MF, Rehman K, Shah MR (2022) Investigation of wound healing potential of photo-active curcumin-ZnO-nanoconjugates in excisional wound model. Photodiagnosis Photodyn Ther 39:102956. https://doi.org/10.1016/j.pdpdt.2022.102956

Baron JM, Glatz M, Proksch E (2020) Optimal Support of Wound Healing: New Insights. Dermatology 236:593–600. https://doi.org/10.1159/000505291

Benakashani F, Allafchian A, Jalali S (2016) Biosynthesis of silver nanoparticles using Capparis spinosa L. leaf extract and their antibacterial activity. Karbala Int J Modern Sci 2:251–258. https://doi.org/10.1016/j.kijoms.2016.08.004

Blanco-Fernandez B, Castano O, Mateos-Timoneda MA, Engel E, Perez-Amodio S (2021) Nanotechnology Approaches in Chronic Wound Healing. Adv Wound Care (new Rochelle) 10:234–256. https://doi.org/10.1089/wound.2019.1094

Caldwell MD (2020) Bacteria and antibiotics in wound healing. Surg Clin 100:757–776. https://doi.org/10.1016/j.suc.2020.05.007

Cui Y, Zhao Y, Tian Y, Zhang W, Lu X, Jiang X (2012) The molecular mechanism of action of bactericidal gold nanoparticles on Escherichia coli. Biomaterials 33:2327–2333. https://doi.org/10.1016/j.biomaterials.2011.11.057

Demir AY, Karadayi M, Hidiroglu N, Dogan S, Bozoglu C, Gulluce M (2016) Bacterial biosynthesis of ZnO nanoparticles from zinc acetate by Rhodococcus erythropolis K85. J Biotechnol 231:S72–S72. https://doi.org/10.1016/j.jbiotec.2016.05.263

Deniz FE (2022) Diabetes mellitus. In: Üstünol D, Ürün Unal B (eds) Chronic Disease Follow-Ups for Adults in Primary Care. Nova Science Publishers Inc., New York, USA, pp 53–69. https://doi.org/10.52305/ONAL5005

Dolivo DM, Larson SA, Dominko T (2017) Fibroblast Growth Factor 2 as an Antifibrotic: Antagonism of Myofibroblast Differentiation and Suppression of Pro-Fibrotic Gene Expression. Cytokine Growth F R 38:49–58. https://doi.org/10.1016/j.cytogfr.2017.09.003

El-Samad LM, Bakr NR, El-Ashram S, Radwan EH, Abdul Aziz KK, Hussein HK, El Wakil A, Hassan MA (2022a) Silver nanoparticles instigate physiological, genotoxicity, and ultrastructural anomalies in midgut tissues of beetles. Chem Biol Interact 367:110166. https://doi.org/10.1016/j.cbi.2022.110166

El-Samad LM, Hassan MA, Basha AA, El-Ashram S, Radwan EH, Abdul Aziz KK, Tamer TM, Augustyniak M, El Wakil A (2022b) Carboxymethyl cellulose/sericin-based hydrogels with intrinsic antibacterial, antioxidant, and anti-inflammatory properties promote re-epithelization of diabetic wounds in rats. Int J Pharm 629:122328. https://doi.org/10.1016/j.ijpharm.2022.122328

Elshama SS, Abdallah ME, Abdel-Karim RI (2018) Zinc oxide nanoparticles: therapeutic benefits and toxicological hazards. Open Nanomed Nanotechnol J 5. https://doi.org/10.2174/1875933501805010016

Ertugrul MS, Nadaroglu H, Nalci OB, Hacimuftuoglu A, Alayli A (2020) Preparation of CoS nanoparticles-cisplatin bio-conjugates and investigation of their effects on SH-SY5Y neuroblastoma cell line. Cytotechnology 72:885–896. https://doi.org/10.1007/s10616-020-00432-5

Ferah Okkay I, Okkay U, Aydin IC, Bayram C, Ertugrul MS, Mendil AS, Hacimuftuoglu A (2022) Centella asiatica extract protects against cisplatin-induced hepatotoxicity via targeting oxidative stress, inflammation, and apoptosis. Environ Sci Pollut Res Int 29:33774–33784. https://doi.org/10.1007/s11356-022-18626-z

Gao Y, Han YY, Cui MY, Tey HL, Wang LH, Xu CJ (2017) ZnO nanoparticles as an antimicrobial tissue adhesive for skin wound closure. J Mater Chem B 5:4535–4541. https://doi.org/10.1039/c7tb00664k

Gharpure S, Ankamwar B (2020) Synthesis and Antimicrobial Properties of Zinc Oxide Nanoparticles. J Nanosci Nanotechnol 20:5977–5996. https://doi.org/10.1166/jnn.2020.18707

Hadley KB, Newman SM, Hunt JR (2010) Dietary zinc reduces osteoclast resorption activities and increases markers of osteoblast differentiation, matrix maturation, and mineralization in the long bones of growing rats. J Nutr Biochem 21:297–303. https://doi.org/10.1016/j.jnutbio.2009.01.002

Harandi FN, Khorasani AC, Shojaosadati SA, Hashemi-Najafabadi S (2021) Living Lactobacillus-ZnO nanoparticles hybrids as antimicrobial and antibiofilm coatings for wound dressing application. Mater Sci Eng C Mater Biol Appl 130:112457. https://doi.org/10.1016/j.msec.2021.112457

Hassan MA, Abd El-Aziz S, Elbadry HM, El-Aassar SA, Tamer TM (2022) Prevalence, antimicrobial resistance profile, and characterization of multi-drug resistant bacteria from various infected wounds in North Egypt. Saudi J Biol Sci 29:2978–2988. https://doi.org/10.1016/j.sjbs.2022.01.015

Hassan MA, Tamer TM, Omer AM, Baset WMA, Abbas E, Mohy-Eldin MS (2023) Therapeutic potential of two formulated novel chitosan derivatives with prominent antimicrobial activities against virulent microorganisms and safe profiles toward fibroblast cells. Int J Pharm 634:122649. https://doi.org/10.1016/j.ijpharm.2023.122649

Hutchings MI, Truman AW, Wilkinson B (2019) Antibiotics: past, present and future. Curr Opin Microbiol 51:72–80. https://doi.org/10.1016/j.mib.2019.10.008

Inam F, Peijs T (2006) Re-aggregation of carbon nanotubes in two-component epoxy system. J Nanostructured Polym Nanocomposites 2:87–95

Jamkhande PG, Ghule NW, Bamer AH, Kalaskar MG (2019) Metal nanoparticles synthesis: An overview on methods of preparation, advantages and disadvantages, and applications. J Drug Deliv Sci Tec 53:101174. https://doi.org/10.1016/j.jddst.2019.101174

Kanda T, Funato N, Baba Y, Kuroda T (2003) Evidence for fibroblast growth factor receptors in myofibroblasts during palatal mucoperiosteal repair. Arch Oral Biol 48:213–221. https://doi.org/10.1016/S0003-9969(02)00204-2

Karaman I, Sahin F, Gulluce M, Ogutcu H, Sengul M, Adiguzel A (2003) Antimicrobial activity of aqueous and methanol extracts of Juniperus oxycedrus L. J Ethnopharmacol 85:231–235. https://doi.org/10.1016/S0378-8741(03)00006-0

Kaushik M, Niranjan R, Thangam R, Madhan B, Pandiyarasan V, Ramachandran C, Oh DH, Venkatasubbu GD (2019) Investigations on the antimicrobial activity and wound healing potential of ZnO nanoparticles. Appl Surf Sci 479:1169–1177. https://doi.org/10.1016/j.apsusc.2019.02.189

Kesmez Can F, Ozkurt Z, Ozturk N, Sezen S (2021) Effect of IL-6, IL-8/CXCL8, IP-10/CXCL 10 levels on the severity in COVID 19 infection. Int J Clin Pract 75:e14970. https://doi.org/10.1111/ijcp.14970

Klink MJ, Laloo N, Leudjo Taka A, Pakade VE, Monapathi ME, Modise JS (2022) Synthesis, Characterization and Antimicrobial Activity of Zinc Oxide Nanoparticles against Selected Waterborne Bacterial and Yeast Pathogens. Molecules 27. https://doi.org/10.3390/molecules27113532

Lemire JA, Harrison JJ, Turner RJ (2013) Antimicrobial activity of metals: mechanisms, molecular targets and applications. Nat Rev Microbiol 11:371–384. https://doi.org/10.1038/nrmicro3028

Liew KB, Janakiraman AK, Sundarapandian R, Khalid SH, Razzaq FA, Ming LC, Khan A, Kalusalingam A, Ng PW (2022) A review and revisit of nanoparticles for antimicrobial drug delivery. J Med Life 15:328–335. https://doi.org/10.25122/jml-2021-0097

Lin P-H, Sermersheim M, Li H, Lee PH, Steinberg SM, Ma J (2017) Zinc in wound healing modulation. Nutrients 10:16. https://doi.org/10.3390/nu10010016

Liu YF, Ni PW, Huang Y, Xie T (2022) Therapeutic strategies for chronic wound infection. Chin J Traumatol 25:11–16. https://doi.org/10.1016/j.cjtee.2021.07.004

Liu Y, Liu YQ, Deng JY, Li W, Nie XQ (2021) Fibroblast Growth Factor in Diabetic Foot Ulcer: Progress and Therapeutic Prospects. Front Endocrinol 12. https://doi.org/10.3389/fendo.2021.744868

Mahmoudvand H, Khaksarian M, Ebrahimi K, Shiravand S, Jahanbakhsh S, Niazi M, Nadri S (2020) Antinociceptive effects of green synthesized copper nanoparticles alone or in combination with morphine. Ann Med Surg (lond) 51:31–36. https://doi.org/10.1016/j.amsu.2019.12.006

Mammadova-Bach E, Braun A (2019) Zinc homeostasis in platelet-related diseases. Int J Mol Sci 20:5258. https://doi.org/10.3390/ijms20215258

Matatkova O, Michailidu J, Miskovska A, Kolouchova I, Masak J, Cejkova A (2022) Antimicrobial properties and applications of

metal nanoparticles biosynthesized by green methods. Biotechnol Adv 58:107905. https://doi.org/10.1016/j.biotechadv.2022.107905
Metwally AA, Abdel-Hady AAA, Haridy MAM, Ebnalwaled K, Saied AA, Soliman AS (2022) Wound healing properties of green (using Lawsonia inermis leaf extract) and chemically synthesized ZnO nanoparticles in albino rats. Environ Sci Pollut Res Int 29:23975–23987. https://doi.org/10.1007/s11356-021-17670-5
Naderi N, Karponis D, Mosahebi A, Seifalian AM (2018) Nanoparticles in wound healing; from hope to promise, from promise to routine. Front Biosci (landmark Ed) 23:1038–1059. https://doi.org/10.2741/4632
Neamah SA, Albukhaty S, Falih IQ, Dewir YH, Mahood HB (2023) Biosynthesis of Zinc Oxide Nanoparticles Using Capparis spinosa L. Fruit Extract: Characterization, Biocompatibility, and Antioxidant Activity. Appl Sci-Basel 13:6604. https://doi.org/10.3390/app13116604
Parveen K, Banse V, Ledwani L (2016) Green Synthesis of Nanoparticles: Their Advantages and Disadvantages. Aip Conf Proc 1724. https://doi.org/10.1063/1.4945168
Penn JW, Grobbelaar AO, Rolfe KJ (2012) The role of the TGF-β family in wound healing, burns and scarring: a review. Int J Burns Trauma 2:18
Rayyif SMI, Mohammed HB, Curutiu C, Birca AC, Grumezescu AM, Vasile BS, Ditu LM, Lazar V, Chifiriuc MC, Mihaescu G, Holban AM (2021) ZnO Nanoparticles-Modified Dressings to Inhibit Wound Pathogens. Materials (Basel) 14. https://doi.org/10.3390/ma14113084
Roberts RE, Cavalcante-Silva J, Kineman RD, Koh TJ (2022) Liver is a primary source of insulin-like growth factor-1 in skin wound healing. J Endocrinol 252:59–70. https://doi.org/10.1530/Joe-21-0298
Samreen AI, Malak HA, Abulreesh HH (2021) Environmental antimicrobial resistance and its drivers: a potential threat to public health. J Glob Antimicrob Resist 27:101–111. https://doi.org/10.1016/j.jgar.2021.08.001
Sezen S, Yeşilyurt F, Özkaraca M, Bayram C, Alaylar B, Güllüce M, Hacımüftüoğlu A (2022) Neuroprotective effect of methanol extract of Capparis spinosa L. fruits in an in-vitro experimental model of Parkinson's disease. J Med Palliat Care 3:341–346. https://doi.org/10.47582/jompac.1198326
Sezen S, Ertuğrul MS, Bayram C, Özkaraca M, Koç TY, Demir AY, Güllüce M, Hacımüftüoğlu A (2023) The in-vitro Wound Healing Potential of Essential Oil Extracted from Mentha longifolia L. J Res Pharm 27. https://doi.org/10.29228/jrp.411
Sharma V, Singh P, Pandey AK, Dhawan A (2012) Induction of oxidative stress, DNA damage and apoptosis in mouse liver after sub-acute oral exposure to zinc oxide nanoparticles. Mutat Res 745:84–91. https://doi.org/10.1016/j.mrgentox.2011.12.009
Sogabe Y, Abe M, Yokoyama Y, Ishikawa O (2006) Basic fibroblast growth factor stimulates human keratinocyte motility by Rac activation. Wound Repair Regen 14:457–462. https://doi.org/10.1111/j.1743-6109.2006.00143.x
Stan D, Tanase C, Avram M, Apetrei R, Mincu NB, Mateescu AL, Stan D (2021) Wound healing applications of creams and "smart" hydrogels. Exp Dermatol 30:1218–1232. https://doi.org/10.1111/exd.14396
Sudhasree S, Banu AS, Brindha P, Kurian GA (2014) Synthesis of nickel nanoparticles by chemical and green route and their comparison in respect to biological effect and toxicity. Toxicol Environ Chem 96:743–754. https://doi.org/10.1080/02772248.2014.923148
Taghizadehghalehjoughi A, Sezen S, Hacimuftuoglu A, Gulluce M (2019) Vincristine combination with Ca(+2) channel blocker increase antitumor effects. Mol Biol Rep 46:2523–2528. https://doi.org/10.1007/s11033-019-04706-w
Taghizadehghalehjoughi A, Sezen S, Bayram C, Hacımüftüoğlu A, Güllüce M (2020) Investigation of anti-tumor effect in neuroblastoma cell line; amlodipine & metformin. Anatol J Bio 1:16–21
Uddin TM, Chakraborty AJ, Khusro A, Zidan BRM, Mitra S, Emran TB, Dhama K, Ripon MKH, Gajdacs M, Sahibzada MUK, Hossain MJ, Koirala N (2021) Antibiotic resistance in microbes: History, mechanisms, therapeutic strategies and future prospects. J Infect Public Health 14:1750–1766. https://doi.org/10.1016/j.jiph.2021.10.020
Vijayakumar V, Samal SK, Mohanty S, Nayak SK (2019) Recent advancements in biopolymer and metal nanoparticle-based materials in diabetic wound healing management. Int J Biol Macromol 122:137–148. https://doi.org/10.1016/j.ijbiomac.2018.10.120
Wang PH, Huang BS, Horng HC, Yeh CC, Chen YJ (2018) Wound healing. J Chin Med Assoc 81:94–101. https://doi.org/10.1016/j.jcma.2017.11.002
WHO (2021) Antimicrobial Resistance. https://www.who.int/news-room/fact-sheets/detail/antimicrobial-resistance. Accessed 9 Sep 2023
Wilkinson HN, Hardman MJ (2020) Wound healing: cellular mechanisms and pathological outcomes. Open Biol 10:200223. https://doi.org/10.1098/rsob.200223
Wuthisuthimethawee P, Lindquist SJ, Sandler N, Clavisi O, Korin S, Watters D, Gruen RL (2015) Wound management in disaster settings. World J Surg 39:842–853. https://doi.org/10.1007/s00268-014-2663-3
Yang H, Liu C, Yang D, Zhang H, Xi Z (2009) Comparative study of cytotoxicity, oxidative stress and genotoxicity induced by four typical nanomaterials: the role of particle size, shape and composition. J Appl Toxicol 29:69–78. https://doi.org/10.1002/jat.1385
Zhang H, Ma ZF (2018) Phytochemical and pharmacological properties of Capparis spinosa as a medicinal plant. Nutrients 10:116. https://doi.org/10.3390/nu10020116

Publisher's Note Springer Nature remains neutral with regard to jurisdictional claims in published maps and institutional affiliations.

Springer Nature or its licensor (e.g. a society or other partner) holds exclusive rights to this article under a publishing agreement with the author(s) or other rightsholder(s); author self-archiving of the accepted manuscript version of this article is solely governed by the terms of such publishing agreement and applicable law.